Available online at www.sciencedirect.com
ScienceDirect
Proceedings of the Combustion Institute 000 (2022) 1–9
Proceedings of the Combustion Institute
www.elsevier.com/locate/proci

Methanol oxidation up to 100 atm in a supercritical pressure jet-stirred reactor

Ziyu Wang [a], Hao Zhao [a,*], Chao Yan [a], Ying Lin [a], Aditya D. Lele [a], Wenbin Xu [a], Brandon Rotavera [b,c], Ahren W. Jasper [d], Stephen J. Klippenstein [d], Yiguang Ju [a]

[a] *Department of Mechanical and Aerospace Engineering, Princeton University, Princeton, NJ 08544, United States of America*
[b] *Department of Chemistry, University of Georgia, Athens, GA 30602, United States of America*
[c] *College of Engineering, University of Georgia, Athens, GA 30602, United States of America*
[d] *Chemical Sciences and Engineering Division, Argonne National Laboratory, Lemont, IL 60439, United States of America*

Received 3 January 2022; accepted 10 July 2022
Available online xxx

Abstract

Methanol (CH_3OH) has attracted considerable attention as a renewable fuel or fuel additive with low greenhouse gas emissions. Methanol oxidation was studied using a recently developed supercritical pressure jet-stirred reactor (SP-JSR) at pressures of 10 and 100 atm, at temperatures from 550 to 950 K, and at equivalence ratios of 0.1, 1.0, and 9.0 in experiments and simulations. The experimental results show that the onset temperature of CH_3OH oxidation at 100 atm is around 700 K, which is more than 100 K lower than the onset at 10 atm and this trend cannot be predicted by the existing kinetics models. Furthermore, a negative temperature coefficient (NTC) behavior was clearly observed at 100 atm at fuel rich conditions for methanol for the first time. To understand the observed temperature shift in the reactivity and the NTC effect, we updated some key elementary reaction rates of relevance to high pressure CH_3OH oxidation from the literature and added some new low-temperature reaction pathways such as $CH_2O + HO_2 = HOCH_2O_2$ (RO_2), $RO_2 + RO_2 = HOCH_2O$ (RO) + $HOCH_2O$ (RO) + O_2, and $CH_3OH + RO_2 = CH_2OH + HOCH_2O_2H$ (ROOH). Although the model with these updates improves the prediction somewhat for the experimental data at 100 atm and reproduces well high-temperature ignition delay times and laminar flame speed data in the literature, discrepancies still exist for some aspects of the 100 atm low-temperature oxidation data. In addition, it was found that the pressure-dependent HO_2 chemistry shifts to lower temperature as the pressure increases such that the NTC effect at fuel-lean conditions is suppressed. Therefore, as shown in the experiments, the NTC phenomenon was only observed at the fuel-rich condition where fuel radicals are abundant

* Corresponding author.
E-mail address: cgsq725525@gmail.com (H. Zhao).

https://doi.org/10.1016/j.proci.2022.07.068

Please cite this article as: Z. Wang, H. Zhao, C. Yan et al., Methanol oxidation up to 100 atm in a supercritical pressure jet-stirred reactor, Proceedings of the Combustion Institute, https://doi.org/10.1016/j.proci.2022.07.068

and the HO_2 chemistry at high pressure is weakened by the lack of oxygen resulting in comparatively little HO_2 formation.

Keywords: Methanol; SP-JSR; Ultra-high pressure; Supercritical pressure; New reactions

1. Introduction

Methanol (CH_3OH) has attracted considerable attention as a renewable fuel or fuel additive for internal combustion engines with low greenhouse gas emissions [1]. Methanol, which is mainly produced from syngas, natural gas [2], and biomass [3] has abundant sources and low cost. Furthermore, a sustainable closed-carbon cycle, where CH_3OH is synthesized from atmospheric carbon dioxide (CO_2) and renewable hydrogen (H_2), was proposed [4]. As the simplest alcohol, CH_3OH is also a critical intermediate species formed in oxygenated fuel and hydrocarbon oxidations and has a supercritical pressure of 82.2 atm, which is very close to typical engine pressures.

Extremely high-pressure combustion is an emerging technique for enhancing thermodynamic efficiency and lowering pollutant emissions [5,6]. Under such high-pressure conditions, multiple-body collisions may cause significant uncertainties of the rate constants calculated using the typical transition state theory. Consequently, the pressure dependency of reaction rates should be re-evaluated for the transition from gas-phase to supercritical conditions. Furthermore, thermodynamic properties and transport properties may deviate significantly from the ideal gas law at ultra-high pressures. Therefore, it is enormously valuable to perform kinetics experiments of CH_3OH oxidation and to develop its chemical kinetic model under extremely high-pressure conditions (above 100 atm).

Unfortunately, there are limited high pressure apparatuses for use in the study of combustion chemistry up to supercritical conditions. Such apparatuses include high-pressure laminar flow reactors [7,8] and high-pressure shock tubes [9,10]. The high-pressure laminar flow reactor is a useful facility for examining high-pressure chemistry. However, due to the "laminar flow" requirement, it needs a long residence time (above 10 s), and the multi-segment temperature heating leads to a non-uniform temperature distribution in the flow direction. As a result, it is very difficult to observe the temperature sensitive negative temperature coefficient (NTC) behavior for engine relevant reaction timescales [11]. Meanwhile, the high-pressure shock tube is usually used for high temperature ignition studies with fast reaction kinetics due to its relatively short residence time (less than 10–20 ms). Therefore, the high-pressure shock tube is not well suited for the study of relatively slow low-temperature chemistry due to wall effects from the shock-boundary layer interaction.

A supercritical pressure jet-stirred reactor (SP-JSR) recently developed by Zhao et al. [12] at Princeton University provides a valuable complement to the high-pressure laminar flow reactor and the high-pressure shock tube for conducting kinetic studies. The SP-JSR operates at a wide range of low temperatures (298–1200 K) and high pressures (10–200 atm) with a well-defined flow residence time (0.1–1.0 s) and a uniform temperature distribution (+/−3 K). We recently studied low- and intermediate-temperature chemistries of n-butane (n-C_4H_{10}) [12] and dimethyl ether (DME) [13] at 100 atm in the SP-JSR. In contrast with a recent study of C_3H_8 oxidation in a laminar flow reactor [11], the NTC behavior can be clearly observed for both n-C_4H_{10} and DME at 100 atm. In addition, the distinctive impact of pressure on the NTC behavior under fuel lean and rich conditions was also demonstrated.

Methanol oxidation was investigated extensively in past decades, including laminar flame speed [14–19], ignition delay time [20–23], and species measurements in laminar flow reactors [24–29] as well as jet-stirred reactors (JSRs) [23,30]. Previous fundamental experiments have been summarized in references [23,31] and will not be reviewed in detail herein. However, experimental data of JSR is still lacking for CH_3OH oxidation at high pressures (above 20 atm). As such, in this work, CH_3OH oxidation experiments at pressures of 10 and 100 atm, at temperatures between 550 and 950 K, and at equivalence ratios of 0.1, 1.0, and 9.0 were performed in our SP-JSR and the resulting data was compared with several existing kinetic models. The mole fractions of CH_3OH, O_2, CO, CO_2, H_2O, CH_2O, and H_2 were measured with a micro-gas chromatograph (μ-GC). The numerical simulations were performed with the Perfectly Stirred Reactor (PSR) module in CHEMKIN software. The effects of pressure on CH_3OH oxidation were investigated at different equivalence ratios. The high-pressure chemistry of CH_3OH was analyzed and the HP-Mech model [32] from Princeton was updated with some new reactions and new rate constants for some important elementary reactions from the literature.

Please cite this article as: Z. Wang, H. Zhao, C. Yan et al., Methanol oxidation up to 100 atm in a supercritical pressure jet-stirred reactor, Proceedings of the Combustion Institute, https://doi.org/10.1016/j.proci.2022.07.068

Table 1
Experimental conditions.

Case	Equivalence ratio	P (atm)	T (K)	CH_3OH (%)	O_2 (%)	N_2 (%)	Residence time (s)
1	0.1	10	550–950	0.4	6	93.6	0.11–0.06
2	1.0	10	550–950	1.93	2.9	95.17	0.11–0.06
3	9.0	10	550–950	2.65	0.45	96.9	0.11–0.06
4	0.1	100	550–950	0.4	6	93.6	0.43–0.25
5	1.0	100	550–950	1.93	2.9	95.17	0.43–0.25
6	9.0	100	550–950	2.65	0.45	96.9	0.43–0.25

Table 2
Updated reaction rate constants. (cf. Table S1 in the Supplementary Material for more information of estimated rate constants).

Reactions	A (cm^3/mol.s)	n	Ea (cal/mol)	Ref.
$H_2O_2 + H \langle=\rangle H_2O + OH$	3.35E+07	1.91	3654	[13]
$H_2O_2\ (+M) \langle=\rangle 2OH\ (+M)$	2.00E+12	0.9	48,749	[13]
LOW	2.49E+24	−2.3	48,749	
TROE	0.43	1.0E-30	1.0E+30	
$HO_2 + HO_2 \langle=\rangle H_2O_2 + O_2$	1.93E-02	4.12	−4960	[36]
$HO_2 + HO_2 \langle=\rangle OH + OH + O_2$	6.41E+17	−1.54	8540	[36]
$CH_3OH + HO_2 \langle=\rangle CH_2OH + H_2O_2$	3.260E+13	0	18,299	[37]
$CH_3OH + HO_2 \langle=\rangle CH_3O + H_2O_2$	1.220E+12	0	20,070.7	[37]
$CH_2O + H\ (+M) \langle=\rangle CH_2OH\ (+M)$	5.40E+11	0.454	3600	[38]
LOW	1.27E+32	−4.82	6530	
TROE	0.7187	1.03E+02	1.291E+03	
$CH_3OH + CH_3O_2 \langle=\rangle CH_2OH + CH_3O_2H$	2.060E-09	6.20	7128.2	[39]
$CH_3OH + CH_3O_2 \langle=\rangle CH_3O + CH_3O_2H$	7.937E-04	4.71	13,560.3	[39]
$CH_3O_2H + (+M) \langle=\rangle CH_3O + OH\ (+M)$	4.05E+19	−1.153	44,250.5	[40]
LOW	3.98E+42	−7.502	46,756.1	
TROE	0.8375	36,562	498.8	
$CH_2O + HO_2 \langle=\rangle HOCH_2O_2$	2.228E+09	0	−1267.9	[41]
$HOCH_2O_2 + HOCH_2O_2 \langle=\rangle HOCH_2O + HOCH_2O + O_2$	3.312E+12	0	0	[42]
$CH_3OH + HOCH_2O_2 \langle=\rangle CH_2OH + HOCH_2O_2H$	3.260E+13	0	13,299.0	Estimated
$CH_3OH + HOCH_2O_2 \langle=\rangle CH_3O + HOCH_2O_2H$	1.220E+12	0	15,070.7	Estimated
$HOCH_2O_2H\ (+M) \langle=\rangle OH + HOCH_2O\ (+M)$	4.05E+19	−1.153	44,250.5	Estimated
LOW	3.89E+42	−7.502	46,756.1	
TROE	0.8375	36,562	498.8	

2. Experimental setup and kinetics models

The schematic setup of our SP-JSR was shown in previous work [12] and Supplementary Material (cf. Fig. S1). The core part is a spherical quartz reactor with an internal volume of 0.4 cm^3. The novelty of the reactor lies in its four special jet fingers with two 0.2 mm inner diameter perpendicular nozzles, which can create intense turbulence and homogenous mixing [33]. Figs. S2 and S3 in the Supplementary Material show the quartz reactor and a schematic of the velocity distribution. The gas flow rates were determined by high-pressure mass flow controllers (Brooks, SLA5800) and the liquid fuel (CH_3OH, Sigma-Aldrich, HPLC Plus, ≥99.9%) was injected into a vaporization line by a high-pressure syringe pump (Harvard PHD). The axial temperature profiles were measured in 1 mm steps along the reactor bulb to verify the uniform temperature distribution (+/−3 K) under experimental conditions. No significant temperature increase, which could change the chemical kinetics, was observed during the measurement. The maximum preheating temperature is lower than the pyrolysis temperature of methanol (~1000 K), which did not affect the reactions of the reactant at the given flow residence time. The details of the heating processes and temperature profile measurement were presented in our previous paper [12]. A quartz sonic nozzle was used to sample the oxidation products exiting from the reactor and the gas samples were quantified with micro gas chromatography (μ-GC). The GC detection limits for selected species are about 20 ppm. The uncertainty of the measured data is about 5%.

Table 1 lists the experimental conditions for the present CH_3OH oxidation measurements. The flow residence time is defined as the ratio of reactor volume to mixture volume flow rate for each temperature and pressure. Instead of keeping the flow residence time constant, the mixture volume flow rate (295 K and 1 atm) was fixed at 1.2 L/min (Cases 1–3) and 3 L/min (Cases 4–6) to reduce errors in flow control and perturbation. Furthermore, the

Please cite this article as: Z. Wang, H. Zhao, C. Yan et al., Methanol oxidation up to 100 atm in a supercritical pressure jet-stirred reactor, Proceedings of the Combustion Institute, https://doi.org/10.1016/j.proci.2022.07.068

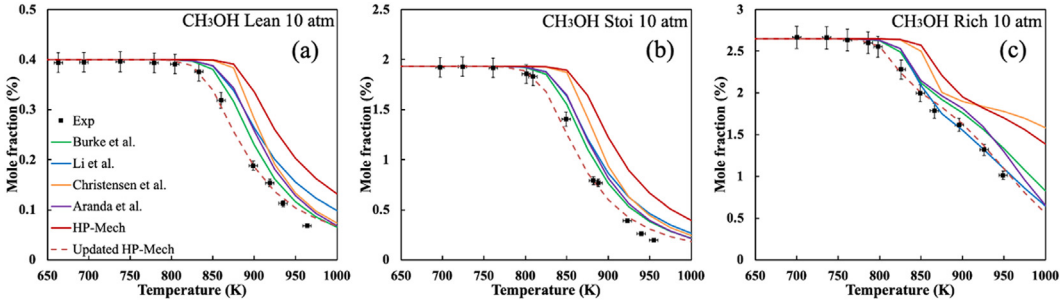

Fig. 1. Temperature evolutions of CH_3OH oxidation: (a) Case 1, (b) Case 2, (c) Case 3 in Table 1 at 10 atm.

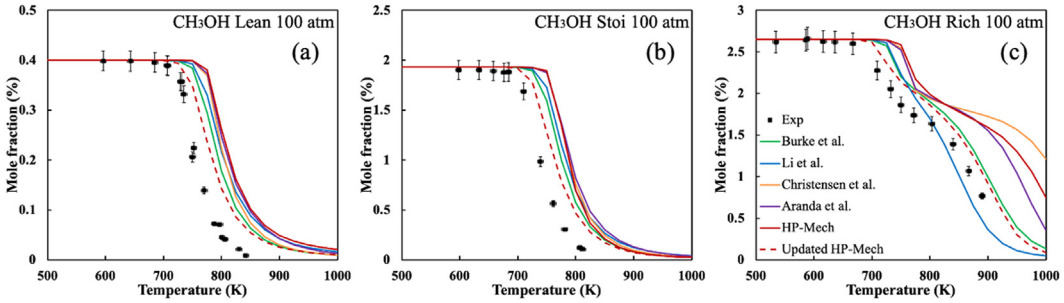

Fig. 2. Temperature evolutions of CH_3OH oxidation: (a) Case 4, (b) Case 5, (c) Case 6 in Table 1 at 100 atm.

flow residence times were selected to correspond with the oxidation reaction time scale (near unity Damköhler number). Each test condition was repeated at least two times to minimize the experimental uncertainty.

The following six kinetic models were used to compare with the experimental data obtained in the SP-JSR: Burke et al. [23], Li et al. [34], Christensen et al. [35], Aranda et al. [29], HP-Mech [32], and an updated HP-Mech (this study, cf. Table 2) [13,36–42]. The numerical simulations were performed with CHEMKIN's PSR module at constant temperature. Calculations indicate that the real gas effect on CH_3OH oxidation is very small even at 100 atm (cf. Fig. S4 in the Supplementary Material).

3. Results and discussion

Fig. 1(a)-(c) depicts the CH_3OH mole fraction evolution versus temperature for case 1 (a), case 2 (b), and case 3 (c) in Table 1 at 10 atm, respectively. It can be noted that the onset temperatures of CH_3OH oxidation at 10 atm are in the range of 800–825 K and that the fuel-rich case (c) has slightly faster oxidation than the fuel-lean case (a). Furthermore, no low-temperature chemistry is found for CH_3OH oxidation at 10 atm, except a small change in curvature at around 850 K brings our attention at fuel-rich case. These results are consistent with the JSR data in literature [23]. As to the numerical simulations at 10 atm, literature models slightly under-predict the CH_3OH oxidation. We updated the rate constants of some key reactions listed in Table 2. The updated HP-Mech model (red dash lines) has very good agreement with the experimental data for temperature up to 900 K. Additionally, the Burke et al., Li et al., and Aranda et al. models can also predict the experimental data reasonably well. The Christensen et al. and HP-Mech models under-predict CH_3OH oxidation, which is mainly due to the uncertainty in the rate of the $CH_3OH + HO_2 = CH_2OH + H_2O_2$ reaction. The rate constant for $CH_3OH + HO_2$ [37] selected in this paper is the one which has the best agreement with the high-pressure experimental data. The recent paper by Li et al. [43] also confirmed this statement. Moreover, more than 150 K difference between the onset temperature of CH_3OH oxidation at 1 and 10 atm was reported in [23], which implies that the pressure-dependent reactions play an important role in CH_3OH oxidation. Therefore, it is very interesting to explore the difference between 10 and 100 atm, especially at fuel-rich condition.

Fig. 2(a)-(c) depicts the CH_3OH mole fraction evolution versus temperature for case 4 (a), case 5 (b), and case 6 (c) in Table 1 at 100 atm, respectively. Experimental results show that the onset temperature of CH_3OH oxidation at 100 atm is around 700 K, which is more than 100 K lower than that

Please cite this article as: Z. Wang, H. Zhao, C. Yan et al., Methanol oxidation up to 100 atm in a supercritical pressure jet-stirred reactor, Proceedings of the Combustion Institute, https://doi.org/10.1016/j.proci.2022.07.068

at 10 atm. Furthermore, a shoulder in the CH_3OH profile is clearly present for the fuel-rich condition at 100 atm. The shoulder in the CH_3OH profile at high pressure represents the remnants of an NTC region, where the fuel oxidation slows down as the temperature is increased. Unlike the cases at 10 atm, all the existing models considered in this work significantly under-predict the oxidation at 100 atm.

In an effort to understand the observed temperature shift in the reactivity and the NTC effect, we updated some key elementary reaction rates from the literature and added some new low-temperature reaction pathways such as $CH_2O + HO_2 = HOCH_2O_2$ (RO_2), $RO_2 + RO_2 = HOCH_2O$ (RO) + HO CH_2O (RO) + O_2, and $CH_3OH + RO_2 = CH_2$ OH + $HOCH_2O_2H$ (ROOH), which are first included in the present methanol model, as listed in Table 2. The updated HP-Mech model (red dash lines) now presents improved agreement with the experimental data. The exact reactions responsible for the changes are H_2O_2 (+M) = 2OH (+M), $CH_2O + HO_2 = HOCH_2O_2$, and CH_3OH + HO $CH_2O_2 = CH_2OH + HOCH_2O_2H$. At higher pressure, the reactions H_2O_2 (+M) = 2OH (+M), $CH_2O + HO_2 = HOCH_2O_2$ play a more important role in methanol oxidation due to the increased collisional energy transfer. These reactions promote the methanol oxidation and result in better agreement with the experimental data. However, discrepancies still exist, especially for the temperature range from 700 to 800 K, which may indicate that a low-temperature, high-pressure reaction pathway is missing and warrants future exploration.

One possible missing pathway could be due to molecular collisions at high pressure thermalizing and stabilizing the excited incipient RO_2 radical. The isomerization reaction $RO_2 = OCH_2O_2H$ (QOOH) and subsequent reactions may promote the CH_3OH oxidation and cause the NTC behavior at high pressure. Another possible reason is that dimer complexes such as $CH_3OH…CH_3OH$, $CH_3OH…HO_2$, and $CH_3OH…H_2O_2$ may play a role at high pressure, especially for fuel-rich condition. That could in principle lower the activation energy barrier for the two most sensitive reactions (cf. Figs. 3 and 4); $CH_3OH…CH_3OH + HO_2 = CH_2OH…H_2O_2$ + CH_3OH, $CH_3OH…HO_2 + CH_3OH = CH_2O$ H…H_2O_2 + CH_3OH and/or $CH_3OH…H_2O_2 = CH_3OH…OH…OH$. The NTC behavior at fuel-rich condition could then be due to the decrease in the dimer complex concentrations at higher temperature, thus decreasing the effectiveness of these pathways.

To explain the pressure effects on CH_3OH oxidation, a reaction pathway analysis was performed for 10 and 100 atm at the onset temperature of the oxidation. The updated HP-Mech model was selected for this analysis based on its superior model performance. Fig. 3(a) and (b) shows the reaction pathway analysis at 725 and 825 K for case 3 and case 6 in Table 1, respectively. It can be noted that the H-abstraction from CH_3OH by OH and HO_2 are very important first-step reactions at both 10 and 100 atm. However, the reaction $CH_3OH + HO_2 = CH_2OH + H_2O_2$ becomes more dominant at higher pressure. This change in importance is due to the dramatic increase in HO_2 production at high pressure, thus, reactions involving HO_2 chemistry have a higher influence on the fuel oxidation. Additionally, the H-abstraction reaction by H also contributes at fuel-rich condition, which is the main channel for H_2 production. The major products of H-abstraction reactions are CH_2OH, CH_3O, and H_2O_2. Nevertheless, the production of CH_2OH is much greater than CH_3O, because the C–H bond on the methyl site is about 9.1 kcal/mol weaker than the alternative O–H bond [23]. Hydrogen peroxide is mainly consumed by the third body reaction H_2O_2 (+M) = 2OH (+M). This branching reaction becomes very important due to the increased collision frequency at high pressure. The major intermediate species in CH_3OH oxidation is CH_2O, which is mainly formed by the reaction $CH_2OH + O_2 = CH_2O + HO_2$. A new reaction $CH_2O + HO_2 = HOCH_2O_2$ (RO_2) is also present here. The reactions related to RO_2 chemistry at high pressure may play an important role in the CH_3OH oxidation and need deeper exploration in the future.

To further investigate the oxidation chemistry of CH_3OH, a sensitivity analysis is performed for CH_3OH mole fractions at two different temperature regions. Fig. 4(a) and (b) present the sensitivity coefficients of major reactions at 100 atm and fuel-rich condition for temperatures of 725 and 775 K, respectively. It can be noted from Fig. 4(a) that the chain-propagating reaction $CH_3OH + HO_2 = CH_2OH + H_2O_2$ is the most sensitive one at the onset temperature of CH_3OH oxidation, which confirms the statement in the reaction pathway analysis. This reaction rate is an important part of the update in this work (Table 2). Moreover, the H-abstraction reaction by OH is of decreased importance at 100 atm, which is also consistent with the reaction pathway analysis. The new reaction $CH_3OH + HOCH_2O_2 = CH_2OH + HOCH_2O_2H$ also essentially promotes the oxidation. The chain-terminating reaction $2HO_2 = H_2O_2 + O_2$ starts to show up at 725 K, which has a large inhibiting effect on the oxidation. This rate constant is also part of the updates in this work (Table 2).

It can also be noted from Fig. 4(b) that the reaction H_2O_2 (+M) = 2OH (+M) becomes the most sensitive one at 775 K. Hydrogen peroxide is mainly formed via reactions $HO_2 + HO_2 = H_2O_2 + O_2$ and

Please cite this article as: Z. Wang, H. Zhao, C. Yan et al., Methanol oxidation up to 100 atm in a supercritical pressure jet-stirred reactor, Proceedings of the Combustion Institute, https://doi.org/10.1016/j.proci.2022.07.068

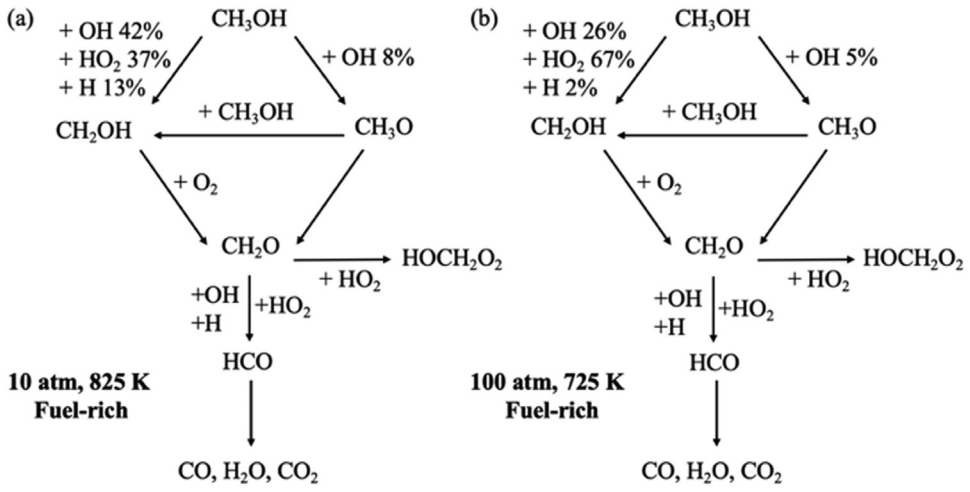

Fig. 3. Reaction pathways for onset of CH_3OH oxidation at (a) 10 atm and (b) 100 atm using the updated HP-Mech model.

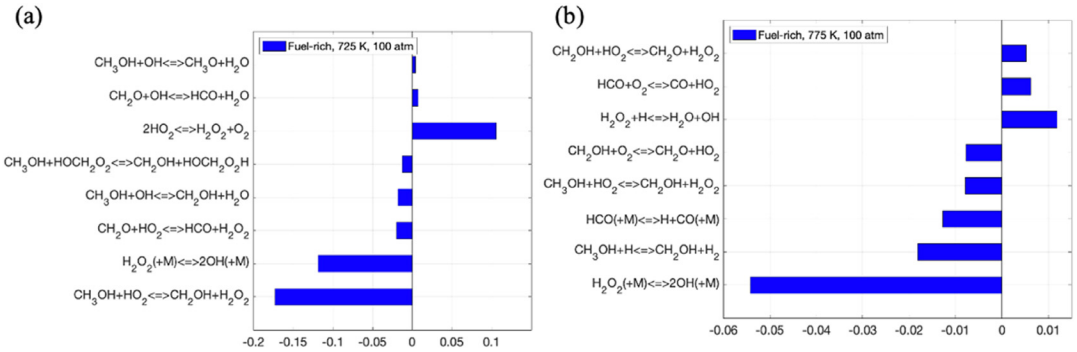

Fig. 4. Sensitivity analysis for CH_3OH oxidation at (a) 725 K and (b) 775 K and 100 atm using updated HP-Mech model.

$CH_3OH + HO_2 = CH_2OH + H_2O_2$. The rate constants of H_2O_2 related reactions are updated in this work (Table 2). The H-abstraction reaction by H becomes more important at this temperature since many H radicals are generated especially for fuel-rich conditions. The abundance of H radicals in the system also yields increased importance for the $H_2O_2 + H = H_2O + OH$ reaction. This reaction has a negative effect on CH_3OH oxidation since it only produces one OH radical while using up the reactive H radical and H_2O_2.

Based on the experimental data in Fig. 2(c), the NTC behavior was clearly observed in the temperature range from 750 to 800 K for fuel-rich condition with abundant R radicals. The NTC behavior could be due to the inhibition of RO_2 formation and its following reactions at higher temperature. Moreover, it could also be caused by the decreasing dimer complex concentrations at higher temperature, thus decreasing the effectiveness of the $CH_3OH\ldots CH_3OH + HO_2 = CH_2OH\ldots CH_3OH + H_2O_2$ pathway, for example. Additionally, HO_2 formation in fuel-rich condition with very low oxygen concentration was much less than that at fuel-lean condition, which inhibits the H_2O_2 formation and downstream chain-branching reaction $H_2O_2 (+M) = 2OH (+M)$. Therefore, at 100 atm the NTC phenomenon can only be observed in fuel-rich condition. This is a unique phenomenon at high pressure.

Fig. 5(a)-(f) illustrates the mole fractions of other key species at 100 atm, such as O_2, CO, CO_2, H_2O, CH_2O, and H_2, respectively. It is seen that the updated HP-Mech model improves the overall prediction compared to other models and the original one, which is consistent with the prediction of CH_3OH consumption. Nevertheless, the model underpredicts CO_2, H_2O, and CH_2O formation and slightly overpredicts H_2 formation. It means the modeling underpredicts the overall reactivity of CH_3OH oxidation. However, the discrepancy between experimental and numerical simulation results for CO_2 production is even bigger than other species. It implies that some important re-

Please cite this article as: Z. Wang, H. Zhao, C. Yan et al., Methanol oxidation up to 100 atm in a supercritical pressure jet-stirred reactor, Proceedings of the Combustion Institute, https://doi.org/10.1016/j.proci.2022.07.068

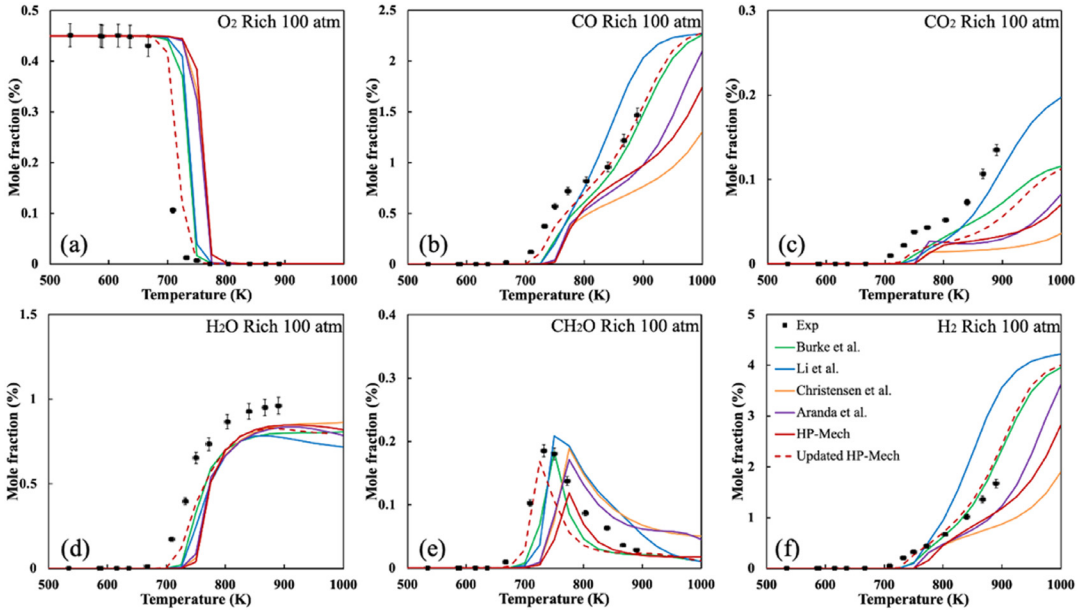

Fig. 5. Temperature evolutions of (a) O_2, (b) CO, (c) CO_2, (d) H_2O, (e) CH_2O, and (f) H_2 mole fractions for fuel-rich condition (Case 6) at 100 atm.

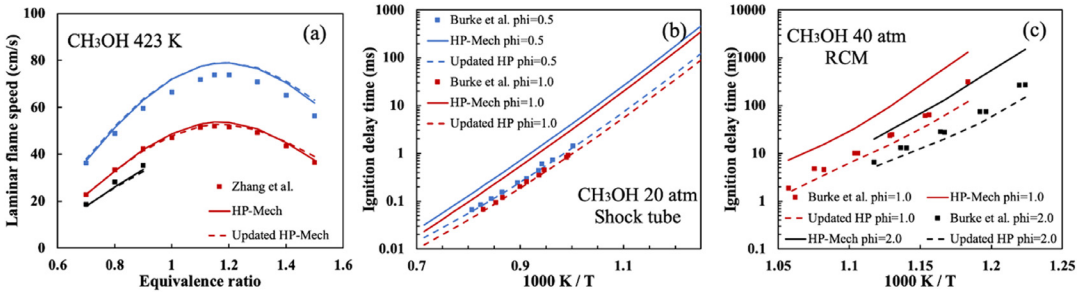

Fig. 6. Comparison of experimental and modeling results for (a) laminar flame speeds of CH_3OH/air with different equivalence ratios at 1, 5, and 10 atm [19]; (b) ignition delay times (shock tube) of CH_3OH/air with different equivalence ratios at 20 atm [23]; (c) ignition delay times (RCM) of $CH_3OH/O_2/N_2/Ar$ with different equivalence ratios at 40 atm [23].

actions involved in CO_2, CO, and HCO, such as $CO + OH = CO_2 + H$, $HCO (+M) = H + CO (+M)$, $HCO + HO_2 = CO_2 + H + OH$, and $CO + HO_2 = CO_2 + OH$ need careful evaluation for ultra-high pressure condition. It is interesting to note that the NTC phenomenon can also be found on the CO and CO_2 production profiles in Fig. 5.

4. Validation of kinetics model with literature data

The updated HP-Mech model is further validated by three sets of literature experimental data: laminar flame speeds [19] and ignition delay times of CH_3OH/oxidizer mixtures measured in a shock tube as well as in a rapid compression machine (RCM) [23]. Fig. 6(a) displays the comparison of experimental laminar flame speed and numerical simulation for different equivalence ratios at different pressures. In general, the experimental and modeling data are in good agreement at different conditions, although the model slightly overpredicts the laminar flame speed at 1 atm. Fig. 6(b) displays the comparison of experimental ignition delay time (shock tube) and numerical simulation for different equivalence ratios and 20 atm. Fig. 6(c) displays the comparison of experimental ignition delay time (RCM) and numerical simulation for different equivalence ratios and 40 atm. Ignition delay times calculated by the updated HP-Mech model are in significantly improved agreement with the experimental data for all conditions.

Please cite this article as: Z. Wang, H. Zhao, C. Yan et al., Methanol oxidation up to 100 atm in a supercritical pressure jet-stirred reactor, Proceedings of the Combustion Institute, https://doi.org/10.1016/j.proci.2022.07.068

5. Conclusions

The supercritical pressure jet-stirred reactor (SP-JSR) provides a new platform for conducting kinetic studies at extreme pressures with a uniform temperature distribution and a short flow residence time. Methanol oxidation was studied at pressures of 10 and 100 atm, temperatures ranging from 550 to 950 K, and equivalence ratios of 0.1, 1.0, and 9.0.

The experimental results show that the onset temperature of CH_3OH oxidation at 100 atm is around 700 K, which is more than 100 K lower than that at 10 atm and cannot be predicted by existing kinetic models. Furthermore, NTC behavior was clearly observed at 100 atm and fuel rich condition.

Several CH_3OH elementary rate constants were updated from the literature and new low-temperature reaction pathways were added to understand the observed reactivity temperature shift and the NTC effect. Although the model with these updates improves the prediction somewhat for the experimental data at 100 atm and reproduces well the ignition delay times and flame speeds data in the literature, discrepancies still exist for low-temperature oxidation. Based on the authors' judgment, these discrepancies cannot be explained by the uncertainty of thermal rate constants for the important existing reactions (e.g. $CH_3OH + HO_2 = CH_2OH + H_2O_2$ and $H_2O_2 (+M) = 2OH (+M)$). These discrepancies reveal that there may be a missing low-temperature high-pressure reaction pathway. Therefore, special attention should be paid to discovering new low-temperature high-pressure reaction pathways. For example, the reaction of dimer complexes needs future exploration.

Furthermore, it was confirmed that the radical production from HO_2 chemistry was significantly enhanced and shifted to lower temperature. As a result, it effectively suppressed the NTC phenomenon for CH_3OH oxidation of lean and stoichiometric mixtures. The NTC phenomenon was only observed at fuel-rich condition because the fuel radicals were increased and the HO_2 chemistry at high pressure was weakened by the lack of oxygen resulting in comparatively little HO_2 formation.

Declaration of Competing Interest

The authors declare that they have no known competing financial interests or personal relationships that could have appeared to influence the work reported in this paper.

Acknowledgments

This work was partly supported by the DOE BES award DE-SC0021135 and the ARO grant W911NF-16-1-0076. The material in this study was partly based on work at ANL supported by the U.S. Department of Energy (USDOE), Office of Basic Energy Sciences, Division of Chemical Sciences, Geosciences, and Biosciences under DOE Contract Number DE-AC02-06CH11357 through the Argonne-Sandia Consortium on High-Pressure Combustion Chemistry, FWP 59044.

Supplementary materials

Supplementary material associated with this article can be found, in the online version, at doi:10.1016/j.proci.2022.07.068.

References

[1] A.K. Agarwal, Biofuels (alcohols and biodiesel) applications as fuels for internal combustion engines, Prog. Energy Combust. Sci 33 (2007) 233–271.
[2] S. Jenkins, Methanol production from natural gas, Chem. Eng. (N.Y.) 123 (2016) 37.
[3] K. Kumabe, S. Fujimoto, T. Yanagida, et al., Environmental and economic analysis of methanol production process via biomass gasification, Fuel 87 (2008) 1422–1427.
[4] G.A. Olah, A. Goeppert, G.K.S. Prakash, Chemical recycling of carbon dioxide to methanol and dimethyl ether: from greenhouse gas to renewable, environmentally carbon neutral fuels and synthetic hydrocarbons, J. Org. Chem. 74 (2009) 487–498.
[5] R.D. Reitz, Combustion and ignition chemistry in internal combustion engines, Int. J. Engine Res. 14 (2013) 411–415.
[6] G.P. Sutton, O. Biblarz, Rocket Propulsion Elements, John Wiley & Sons, 2016.
[7] C.L. Rasmussen, J. Hansen, P. Marshall, P. Glarborg, Experimental measurements and kinetic modeling of CO/H2/O2/NOx conversion at high pressure, Int. J. Chem. Kinet. 40 (2008) 454–480.
[8] R.X. Fernandes, K. Luther, J. Troe, Falloff curves for the reaction CH3 + O2 (+ M) → CH3O2 (+ M) in the pressure range 2−1000 bar and the temperature range 300−700 K, J. Phys. Chem. A 110 (2006) 4442–4449.
[9] J. Shao, R. Choudhary, D.F. Davidson, et al., Ignition delay times of methane and hydrogen highly diluted in carbon dioxide at high pressures up to 300 atm, Proc. Combust. Inst. 37 (2019) 4555–4562.
[10] G. Kogekar, C. Karakaya, G.J. Liskovich, et al., Impact of non-ideal behavior on ignition delay and chemical kinetics in high-pressure shock tube reactors, Combust. Flame 189 (2018) 1–11.
[11] H. Hashemi, J.M. Christensen, L.B. Harding, S.J. Klippenstein, P. Glarborg, High-pressure oxidation of propane, Proc. Combust. Inst. 37 (2019) 461–468.
[12] H. Zhao, C. Yan, T. Zhang, et al., Studies of high-pressure n-butane oxidation with CO2 dilution up to 100 atm using a supercritical-pressure jet-stirred reactor, Proc. Combust. Inst. 38 (2021) 279–287.
[13] C. Yan, H. Zhao, Z. Wang, et al., Low- and intermediate-temperature oxidation of dimethyl ether up to 100 atm in a supercritical pressure jet-stirred reactor, Combust. Flame (2022) 112059 in press.

Please cite this article as: Z. Wang, H. Zhao, C. Yan et al., Methanol oxidation up to 100 atm in a supercritical pressure jet-stirred reactor, Proceedings of the Combustion Institute, https://doi.org/10.1016/j.proci.2022.07.068

[14] S.Y. Liao, D.M. Jiang, Z. Huang, K. Zeng, Characterization of laminar premixed methanol-air flames, Fuel 85 (2006) 1346–1353.
[15] Z. Zhang, Z. Huang, X. Wang, et al., Measurements of laminar burning velocities and Markstein lengths for methanol-air-nitrogen mixtures at elevated pressures and temperatures, Combust. Flame 155 (2008) 358–368.
[16] P.S. Veloo, Y.L. Wang, F.N. Egolfopoulos, C.K. Westbrook, Comparative experimental and computational study of methanol, ethanol, and n-butanol flames, Combust. Flame 157 (2010) 1989–2004.
[17] J. Vancoillie, M. Christensen, E.J.K. Nilsson, et al., Temperature dependence of the laminar burning velocity of methanol flames, Energy Fuel. 26 (2012) 1557–1564.
[18] J. Beeckmann, L. Cai, H. Pitsch, Experimental investigation of the laminar burning velocities of methanol, ethanol, n-propanol, and n-butanol at high pressure, Fuel 117 (2014) 340–350.
[19] X. Zhang, G. Wang, J. Zou, et al., Investigation on the oxidation chemistry of methanol in laminar premixed flames, Combust. Flame 180 (2017) 20–31.
[20] K. Fieweger, R. Blumenthal, G. Adomeit, Self-Ignition of S.I. engine model fuels: a shock tube investigation at high pressure, Combust. Flame 109 (1997) 599–619.
[21] K.E. Noorani, B. Akih-Kumgeh, J.M. Bergthorson, Comparative high temperature shock tube ignition of C1–C4 primary alcohols, Energy Fuels 24 (2010) 5834–5843.
[22] K. Kumar, C.J. Sung, Autoignition of methanol: experiments and computations, Int. J. Chem. Kinet. 43 (2011) 175–184.
[23] U. Burke, W.K. Metcalfe, S.M. Burke, et al., A detailed chemical kinetic modeling, ignition delay time and jet-stirred reactor study of methanol oxidation, Combust. and Flame 165 (2016) 125–136.
[24] T.S. Norton, F.L. Dryer, Some new observations on methanol oxidation chemistry, Combust. Sci. Technol 63 (1989) 107–129.
[25] T.J. Held, F.L. Dryer, An experimental and computational study of methanol oxidation in the intermediate and high-temperature regimes, Symp. (Int.) Combust. 25 (1994) 901–908.
[26] M.U. Alzueta, R. Bilbao, M. Finestra, Methanol oxidation and its interaction with nitric oxide, Energy Fuel. 15 (2001) 724–729.
[27] W.-.C. Ing, C.Y. Sheng, J.W. Bozzelli, Development of a detailed high-pressure reaction model for methane/methanol mixtures under pyrolytic and oxidative conditions and comparison with experimental data, Fuel Proc. Technol. 83 (2003) 111–145.
[28] C.L. Rasmussen, K.H. Wassard, K. Dam-Johansen, P. Glarborg, Methanol oxidation in a flow reactor: implications for the branching ratio of the CH3OH + OH reaction, Int. J. Chem. Kinet 40 (2008) 423–441.
[29] V. Aranda, J.M. Christensen, M.U. Alzueta, et al., Experimental and kinetic modeling study of methanol ignition and oxidation at high pressure, Int. J. Chem. Kinet. 45 (2013) 283–294.
[30] G. Dayma, K.H. Ali, P. Dagaut, Experimental and detailed kinetic modeling study of the high-pressure oxidation of methanol sensitized by nitric oxide and nitrogen dioxide, Proc. Combust. Inst. 31 (2007) 411–418.
[31] S.M. Sarathy, P. Oßwald, N. Hansen, K. Kohse-Höinghaus, Alcohol combustion chemistry, Prog. Energ. Combust. Sci 44 (2014) 40–102.
[32] C. Reuter, R. Zhang, O. Yehia, Y. Rezgui, Y. Ju, Counterflow flame experiments and chemical kinetic modeling of dimethyl ether/methane mixtures, Combust. Flame 196 (2018) 1–10.
[33] H. Zhao, M. Souza, Y. Ju, Fusion, J. Am. Sci. Glassblower. Soc. 66 (2018) 19–24.
[34] J. Li, Z. Zhao, A. Kazakov, M. Chaos, F.L. Dryer, J.J. Scire Jr, A comprehensive kinetic mechanism for CO, CH2O, and CH3OH combustion, Int. J. Chem. Kinet. 39 (2007) 109–136.
[35] M. Christensen, E.J.K. Nilsson, A.A. Konnov, A systematically updated detailed kinetic model for CH_2O and CH_3OH combustion, Energy Fuel. 30 (2016) 6709–6726.
[36] S.J. Klippenstein, R. Sivaramakrishnan, U. Burke, et al., HO_2+HO_2: high level theory and the role of singlet channels, Combust. Flame (2022) 111975 in press.
[37] M. Altarawneh, A.H. Al-Muhtaseb, B.Z. Dlugogorski, et al., Rate constants for hydrogen abstraction reactions by the hydroperoxyl radical from methanol, ethenol, acetaldehyde, toluene, and phenol, J. Comp. Chem. 32 (2011) 1725–1733.
[38] A. Laskin, H. Wang, C.K. Law, Detailed kinetic modeling of 1,3-butadiene oxidation at high temperatures, Int. J. Chem. Kinet. 32 (2000) 589–614.
[39] Z. Zhao, J. Song, B. Su, X. Wang, Z. Li, Mechanistic study of the reactions of methyl peroxy radical with methanol or hydroxyl methyl radical, J. Phys. Chem. A 122 (2018) 5078–5088.
[40] A.W. Jasper, S.J. Klippenstein, L.B. Harding, Theoretical rate coefficients for the reaction of methyl radical with hydroperoxyl radical and for methylhydroperoxide decomposition, Proc. Combust. Inst. 32 (2009) 279–286.
[41] P. Morajkar, C. Schoemaecker, M. Okumura, C. Fittschen, Direct measurement of the equilibrium constants of the reaction of formaldehyde and acetaldehyde with HO2 radicals, Int. J. Chem. Kinet. 46 (2014) 245–259.
[42] R. Atkinson, D.L. Baulch, R.A. Cox, J.N. Crowley, R.F. Hampson, R.G. Hynes, M.E. Jenkin, J.A. Kerr, M.J. Rossi, J. Troe, Summary of Evaluated Kinetic and Photochemical Data for Atmospheric Chemistry, IUPAC Subcommittee on Gas Kinetic Data Evaluation for Atmospheric Chemistry, 2006, http://www.iupac-kinetic.ch.cam.ac.uk.
[43] G. Li, H. Hashemi, P. Glarborg, Y. Lu, A kinetic model for high-pressure methanol oxidation in gas phase and supercritical water, Energy Fuel. 36 (2022) 575–588.

Please cite this article as: Z. Wang, H. Zhao, C. Yan et al., Methanol oxidation up to 100 atm in a supercritical pressure jet-stirred reactor, Proceedings of the Combustion Institute, https://doi.org/10.1016/j.proci.2022.07.068